

Characteristics of Magnetic Fluctuations during Magnetic Reconnection in Counter-Helicity Spheromak Merging Experiment^{*)}

Ryoma YANAI, Akihiro KUWAHATA¹⁾ and Michiaki INOMOTO¹⁾

Graduate School of Engineering, The University of Tokyo, Bunkyo, Tokyo 113-0032, Japan

¹⁾*Graduate School of Frontier Sciences, The University of Tokyo, Kashiwa, Chiba 277-8561, Japan*

(Received 30 November 2015 / Accepted 12 February 2016)

We performed detailed magnetic probe measurement to detect magnetic fluctuations during magnetic reconnection in counter-helicity spheromak merging experiment in TS-4. The fluctuation power in the frequency range of 0.5 - 5 MHz was concentrated in the outboard-side downstream region of the reconnection point while the fluctuation power in the frequency range of 7 - 20 MHz was localized inside the current sheet. It has been found that the detected fluctuations inside the current sheet had similar characteristics to obliquely propagating Whistler waves, but showed different power spectra inside the current sheet and in the downstream region.

© 2016 The Japan Society of Plasma Science and Nuclear Fusion Research

Keywords: magnetic reconnection, magnetic fluctuation, Whistler wave, spheromak merging

DOI: 10.1585/pfr.11.2401069

1. Introduction

Magnetic reconnection [1] is an elementary process causing magnetic topology change and magnetic energy release in a variety of magnetized plasmas. A two-dimensional steady model of magnetic reconnection proposed by Sweet and Parker [2, 3] provided a quantitative prediction of reconnection rate for the first time, but it could not interpret the eruptive reconnection events, e.g. solar flares. In those fast reconnection cases, the effective resistivity should be enhanced inside the diffusion region. Fluctuations have been considered to be one of the origins of this anomalous resistivity [4] and intensively studied in space observation, numerical studies and laboratory experiments. In particle-in-cell simulation study [5], it was predicted that Whistler waves are excited due to the electron pressure anisotropy in the downstream region, but they didn't contribute to the electron dissipation in the diffusion region. On the other hand, Whistler-like electromagnetic fluctuations were observed in the center of the current sheet of anti-parallel reconnection in a laboratory experiment [6]. In this case, the electromagnetic fluctuation was supposed to be driven by the modified two-stream instability and showed a positive relation with the reconnection rate.

Fast reconnection was also observed in the counter-helicity magnetic reconnection but the mechanisms for the enhancement of reconnection rate is not clear [7]. Previous our experiment reports that low-frequency magnetic fluctuations in the ion-cyclotron frequency range were de-

tected during counter-helicity spheromak merging in TS-3 [8]. However, the fluctuations influence not the fast reconnection but the ion heating. The experiments reported here were performed in TS-4 plasma merging device. We report, in this paper, experimental results on the spatial distribution and spectral structure of the electromagnetic fluctuations generated during reconnection, and the relation between the reconnection rate and the fluctuation amplitudes.

2. Experimental Setup

TS-4 has a cylindrical vacuum vessel made of stainless steel with a diameter of 1600 mm and a total length of 1600 mm. Two spheromaks were generated by two flux cores which are located symmetrically with respect to the midplane ($z = 0$ mm) inside of the vacuum vessel and contain a poloidal magnetic field coil and a toroidal magnetic field coil. After the spheromaks are pinched off from the flux cores, they approach together and merge into one through magnetic reconnection. When the spheromaks have the same polarities of toroidal magnetic field, only poloidal magnetic field reconnects (co-helicity spheromak merging). On the other hand, when the polarities of toroidal magnetic field of the spheromaks are opposite, reconnection of both poloidal and toroidal magnetic field takes place (counter-helicity spheromak merging). Furthermore, counter-spheromak merging can be classified into two types, Case-O and Case-I. The type that toroidal field polarity of spheromak on positive z -side is positive corresponds to Case-O and the opposite one is Case-I [7]. In this experiment, we adopted Case-O. Global 2-D structures of poloidal magnetic flux and toroidal electric field

author's e-mail: yanai@ts.t.u-tokyo.ac.jp

^{*)} This article is based on the presentation at the 25th International Toki Conference (ITC25).

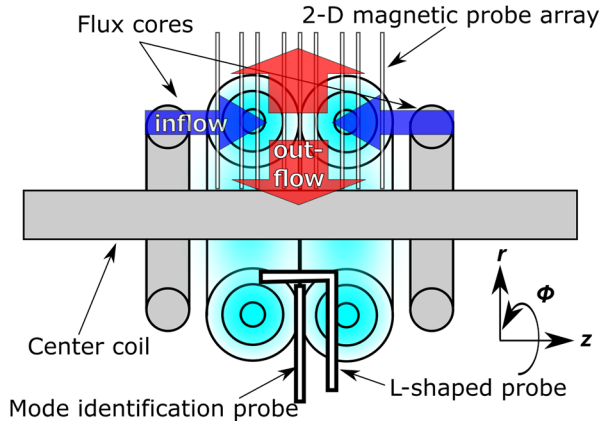


Fig. 1 Schematic view of spheromak merging experiment in TS-4 and experimental setup of 2-D magnetic probe array and magnetic fluctuation probes. Blue and red arrows indicate the direction of reconnection inflows and outflows in this experiment, respectively.

are derived from 2-D magnetic probe array which measures axial and toroidal magnetic field components at 9×10 points in the r - z plane. Poloidal magnetic flux Ψ and toroidal electric field E_ϕ are calculated as following equations:

$$\Psi = \int_{r_{\min}}^r 2\pi r' B_z dr', \quad (1)$$

$$E_\phi = -\frac{1}{2\pi r} \frac{\partial \Psi}{\partial t}. \quad (2)$$

Figure 1 indicates a schematic view of this experiment. L-shaped probe and mode identification probe, which are constructed with the same pickup coils, were inserted at $z = 130$ mm and $z = 0$ mm on the same poloidal plane respectively to measure the reconnection event which takes place on the midplane. Those probes were employed in this experiment to identify the spatial structure and dispersion relation of magnetic fluctuations ($\tilde{B} = \partial B / \partial t$). L-shaped magnetic fluctuation probe consists of 15ch radial and toroidal components ($\tilde{B}_r, \tilde{B}_\phi$) and 13ch axial components (\tilde{B}_z) and can measure the axial distribution of three components of magnetic fluctuations with minimal spatial interval 10 mm.

Mode identification probe mounts three large coils to measure three components of ambient magnetic field (B_r, B_ϕ, B_z) and six small coils to measure magnetic fluctuations. Three of them measure three directional components ($\tilde{B}_r, \tilde{B}_\phi, \tilde{B}_z$). The rest of them are three axial components (\tilde{B}_z) to detect a propagating direction of the fluctuations. The phase difference of each frequency is computed by cross-spectral density (CSD)

$$\theta(\omega) = \arctan\left(\frac{\Im(\text{CSD})}{\Re(\text{CSD})}\right), \quad (3)$$

where $\theta(\omega)$ is a phase difference and \Im indicates imaginary part and \Re indicates real part of CSD. θ is also expressed

as

$$\theta(\omega) = k\Delta x - \omega\Delta t, \quad (4)$$

where Δx is the distance between the reference and the neighboring axial coils, ω is an angular frequency of a wave and Δt is a time difference. The spatial difference of radial and toroidal direction is 1.5 mm and that of axial direction is 0.85 mm in the mode identification probe. In this measurement, the phase difference is caused by not the time difference but the space difference. Therefore, the wavenumber is obtained as a function of angular frequency:

$$k = \frac{\theta(\omega)}{\Delta x}. \quad (5)$$

3. Experimental Results

Magnetic fluctuations were observed during counter-helicity spheromak merging experiment in TS-4, in which the X-point located at about $r = 450$ mm. Figures 2 (a) and (b) indicate typical \tilde{B}_ϕ signals measured by L-shaped probe and their wavelet power spectrums of the fluctuations at each location respectively. We measured significant magnetic fluctuations at $r = 550$ mm (outboard side downstream region) and $r = 450$ mm (inside the current sheet) while we could detect no distinctive fluctuations at $r = 350$ mm (inboard side downstream region). Figure 2 (c) shows ensemble averaged reconnection electric field calculated from 2-D magnetic probe array and magnetic reconnection takes place in $t \sim 500$ - 535 μ s. Both signals observed at $r = 550$ mm and 450 mm clearly showed that magnetic fluctuations with the frequency of 1 - 10 MHz were driven during reconnection. Especially, the higher frequency fluctuations with $f > 7$ MHz were detected only in the vicinity of the X-point, while the lower frequency fluctuations with $f = 1$ - 5 MHz were more significant in the outboard downstream region. The radial component \tilde{B}_r signals were found to be similar to the toroidal component. We measured the spatial distribution of magnetic fluctuations by scanning the L-shaped probe from $r = 350$ mm to $r = 650$ mm. Figure 3 (a) shows the spatial distribution of magnetic fluctuation power on r - z plane with the frequency range of 0.5 - 5 MHz and Fig. 3 (b) shows that with the frequency range of 7 - 20 MHz. We found that the higher frequency fluctuation was localized inside the current sheet. On the other hand, the lower frequency fluctuations were significant in the outboard side downstream region. It is noted that the X-point moved in the radial direction during reconnection. However, the radial motion of the X-point is relatively small compared with the gap between the locations that two distinct frequency fluctuations were observed.

Figure 4 indicates relations between calculated wavenumber and frequency obtained by the mode identification probe located inside the current sheet. In these plots, data from several tens of discharges were included. Horizontal axis of Fig. 4 (a) is radial wavenumber k_r and

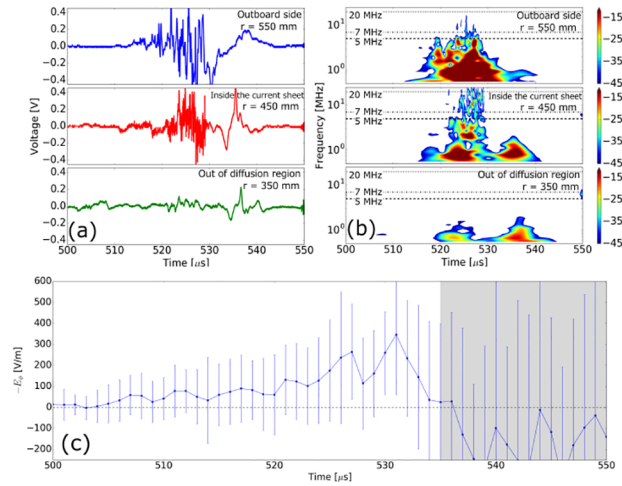


Fig. 2 (a) Typical magnetic fluctuation \vec{B}_ϕ signals measured by L-shaped probe at different radial points on the midplane, (top) $r = 550$ mm, (middle) $r = 450$ mm and (bottom) $r = 350$ mm and (b) wavelet power spectrums of each fluctuation signal. (c) Averaged toroidal electric field E_ϕ at X-point calculated from 2-D magnetic probe array. Magnetic reconnection takes place in $t \sim 500 - 535$ μ s in most discharges, then the merged plasma rapidly decays after reconnection represented by the gray shaded area ($t > 535$ μ s).

those of Figs. 4(b), (c) and (d) are toroidal wavenumber k_ϕ , axial wavenumber k_z and total (L_2 norm) wavenumber $|k|$, respectively. Clear trends are found in dispersion relations on both radial and toroidal wavenumbers while axial wavenumber plot is indistinctive. We found that the fluctuations observed inside the current sheet had large negative wavenumber in the radial direction and small wavenumber in toroidal direction. Dispersion relation of total wavenumber was similar to that of radial wavenumber. Theoretical dispersion relations of Whistler wave traveling with angles ψ with regard to the ambient magnetic field of 10 mT and plasma density of $5 \times 10^{19} \text{ m}^{-3}$ are also plotted in Fig. 4(d). The direction of the ambient magnetic field which was almost on $r - \phi$ plane inside the current sheet. The wavenumber and the frequency of the magnetic fluctuations measured inside the current sheet were comparable with those of Whistler waves and it can be considered that the measured fluctuations were obliquely propagating Whistler waves. The dispersion relation measured at the outboard side downstream region has a similar trend with those observed inside the current sheet.

Figure 5 indicates ensemble averaged sum of power spectral density (PSD) of three components of magnetic fluctuations ($\vec{B}_r, \vec{B}_\phi, \vec{B}_z$) inside the current sheet and the outflow region of outboard side and each noise level, which were calibrated by the frequency response of the mode identification probe. PSD of the fluctuations inside the current sheet had distinctive PSD in the frequency of over 7 MHz compared to that of the outboard side. Both fluctu-

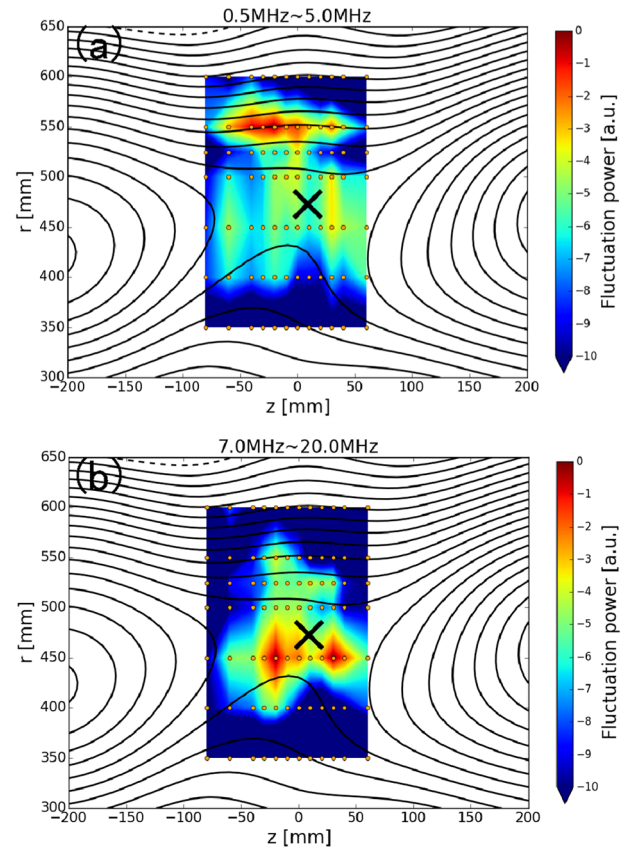


Fig. 3 Spatial distribution of magnetic fluctuation power of (a) 0.5 - 5 MHz and (b) 7 - 20 MHz components. Orange dots indicate measurement points and cross mark represents the X-point. Each power was calculated from the fluctuation signals during 515 - 535 μ s. Black lines illustrate the poloidal magnetic flux contour at $t = 528$ μ s.

ations had broad power spectra and followed different frequency power laws. The fluctuations with the frequency of 1 - 5 MHz showed spectrum shape of $f^{-1.29}$ in the outboard side and $f^{-0.9}$ inside the current sheet.

4. Discussion

We clarified that different types of magnetic fluctuations exist in current sheet and the outboard side downstream region during reconnection in counter-helicity spheromak merging experiment. The fluctuations inside the current sheet had distinctive power in the higher frequency range than in the downstream region and it is conjectured that this mode is directly excited by modified two-stream instability as reported in the experiment of antiparallel reconnection [6]. However, there are no clear relations between the maximum value of magnetic fluctuation and that of reconnection electric field in this experiment.

Though the detected fluctuations are distinguished into two frequency parts in their spectra, no remarkable change was observed in their dispersion relations. Thus, those two parts are supposed to belong to the same branch of obliquely propagating Whistler waves. The wave vec-

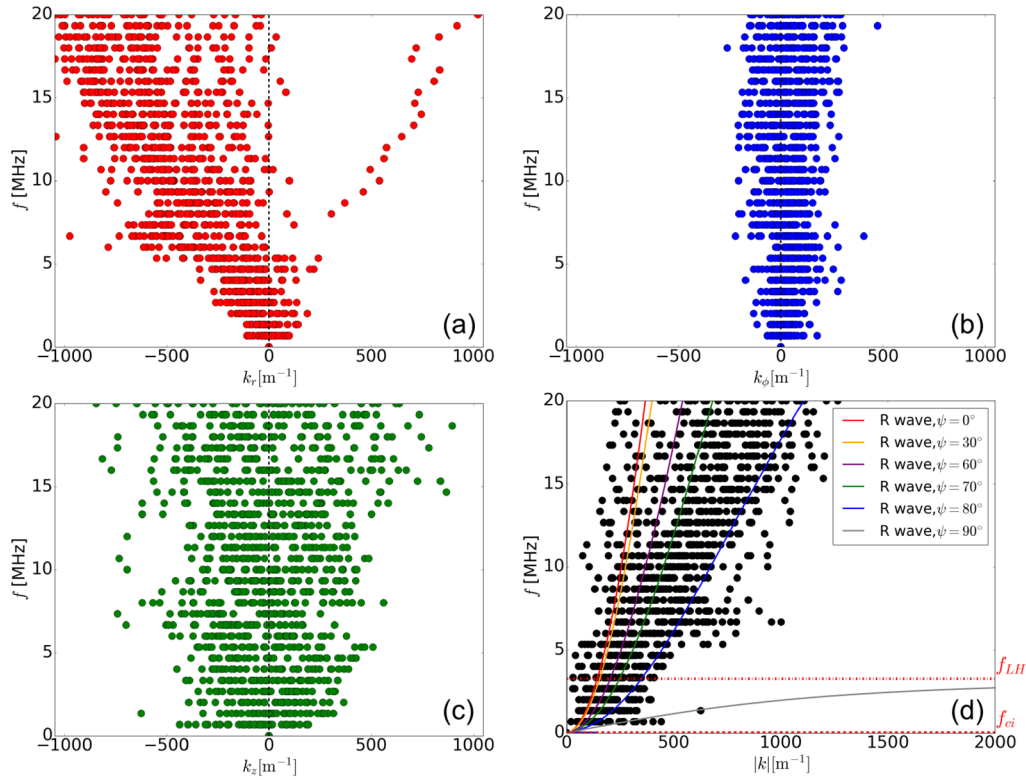


Fig. 4 Dispersion relations of the fluctuations observed inside the current sheet in different horizontal axis of (a) k_r , (b) k_ϕ , (c) k_z and (d) $|k| = \sqrt{k_r^2 + k_\phi^2 + k_z^2}$ with R-wave relations at $B = 10$ mT and $n_e = 5.0 \times 10^{19} \text{ m}^{-3}$ in different angles formed by propagating direction and ambient magnetic field. Red dotted line and dashed line indicate ion cyclotron frequency and lower-hybrid frequency respectively. Each dispersion relation was calculated during the $15 \mu\text{s}$ when the fluctuations were observed.

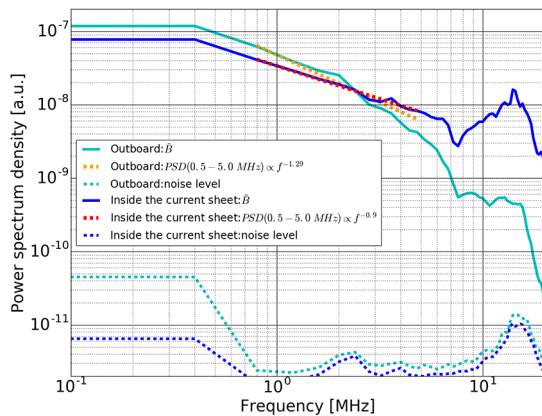


Fig. 5 Ensemble averaged total power spectral density (PSD) of magnetic fluctuations ($\tilde{B}_r, \tilde{B}_\phi, \tilde{B}_z$) measured at different radial points of (blue) inside the current sheet and (cyan) outboard side. Dotted lines indicate noise level at each point. Red and orange dotted lines are fitted line of PSD inside the current sheet and that in the outboard side from 0.5 to 5 MHz, respectively. Those PSD are calibrated by the probe frequency response. Each PSD was calculated during the $15 \mu\text{s}$ when the fluctuations were observed.

tor of fluctuations directs mostly inward radial direction, indicating that they propagate towards the inboard side. Considering the fact that the lower frequency component

had large power in the outboard side downstream region, it is conjectured that these fluctuations are driven in the outboard side downstream region and counter flow against the reconnection outflow. In fact, since the current sheet tilts from a poloidal plane and the direction of electron drift motion is not only toroidal but also radial outward in Case-O, modified two-stream instability could be generated in the outboard side rather than inside the current sheet. Therefore, the larger amplitude fluctuations were detected is not the inboard side but those regions.

Calculated PSD in Fig. 5 indicates the power of $\partial B / \partial t$. Dividing PSD by f^2 , we can derive PSD of the same dimension with B^2 . The estimated power law of PSD of magnetic field fluctuation was $f^{-2.9}$ inside the current sheet and $f^{-3.29}$ in the outboard side. Power law of fluctuations inside the current sheet was close to the Hall MHD turbulence power law of $f^{-7/3}$ [9]. We consider that the higher frequency magnetic fluctuations were generated in the vicinity of the diffusion region, making the slope of the spectrum shallower possibly by the inverse cascade.

5. Conclusion

We carried out detailed probe measurement to observe magnetic fluctuations during counter-helicity spheromak merging. Two distinct frequency components were ob-

served during reconnection. The lower frequency component was concentrated in the outboard-side downstream region of reconnection site while the higher frequency component was localized inside the current sheet. The fluctuations had characteristics like Whistler wave and are supposed to be driven at different locations. Although the observed fluctuations had no clear relation with fast reconnection, it is expected that the fluctuations play an important role such as electron heating [10].

Acknowledgements

This work was supported by JSPS A3 Foresight Program “Innovative Tokamak Plasma Startup and Current Drive in Spherical Torus”, Giant-in Aid for Scientific Research (KAKENHI) 15H05750, 15K14279, 26287143 and the NIFS Collaboration Research program (NIFS14KNWP004).

- [1] M. Yamada, R. Kulsrud and H. Ji, *Rev. Mod. Phys.* **82**, No.1, 603 (2010).
- [2] P.A. Sweet, *Electromagnetic Phenomena in Cosmical Physics*, edited by Bo Lehnert (Cambridge University Press, 1958) p.123.
- [3] E.N. Parker, *J. Geophys. Res.* **62**, 509 (1957).
- [4] R. Kulsrud, H. Ji, W. Fox and M. Yamada, *Phys. Plasmas* **12**, 082301 (2005).
- [5] K. Fujimoto and R. Sydra, *Geophys. Res. Lett.* **35**, L19112 (2008).
- [6] H. Ji, S. Terry, M. Yamada, R. Kulsrud, A. Kuritsyn and Y. Ren, *Phys. Rev. Lett.* **92**, 115001 (2004).
- [7] M. Inomoto, S.P. Gerhardt, M. Yamada, H. Ji, E. Belova, A. Kuritsyn and Y. Ren, *Phys. Rev. Lett.* **97**, 135002 (2006).
- [8] A. Kuwahata, H. Tanabe, S. Ito, M. Inomoto and Y. Ono, *IEEJ Trans. FM* **132**, No.3, 233 (2012).
- [9] M.R. Brown, D.A. Schaffner and P.J. Weck, *Phys. Plasmas* **22**, 055601 (2015).
- [10] X. Tang, C. Cattell, J. Dombeck, L. Dai, L.B. Wilson III, A. Breneman and A. Hupach, *Geophys. Res. Lett.* **40**, 2884 (2013).